Nuclear Correlations and the *r* Process

A. Arcones*

Department of Physics, University of Basel, Klingelbergstraße 82, CH-4056, Switzerland
Institut für Kernphysik, Technische Universität Darmstadt, Schlossgartenstraße 2, D-64289 Darmstadt, Germany
GSI Helmholtzzentrum für Schwerionenforschung GmbH, Planckstrasse 1, D-64291 Darmstadt, Germany

G. F. Bertsch

Department of Physics and Institute for Nuclear Theory, Box 351560, University of Washington, Seattle, Washington 98915, USA
(Received 21 November 2011; published 13 April 2012)

We show that long-range correlations for nuclear masses have a significant effect on the synthesis of heavy elements by the *r* process. As calculated by Delaroche *et al.* [Phys. Rev. C **81**, 014303 (2010)], these correlations suppress magic number effects associated with minor shells. This impacts the calculated abundances before the third *r*-process peak (at mass number $A \approx 195$), where the abundances are low and form a trough. This trough and the position of the third abundance peak are strongly affected by the masses of nuclei in the transition region between deformed and spherical. Based on different astrophysical environments, our results demonstrate that a microscopic theory of nuclear masses including correlations naturally smoothens the separation energies, thus reducing the trough and improving the agreement with observed solar system abundances.

DOI: 10.1103/PhysRevLett.108.151101 PACS numbers: 26.30.Hj, 21.10.Dr, 21.60.Jz

The rapid neutron-capture process (*r* process) leads to half of the nuclei heavier than iron. In this nucleosynthesis process many neutrons are captured by seed nuclei (i.e., iron group and nuclei up to $A \approx 90$) in time scales shorter than β decay. The pathway for the *r* process thus involves extremely neutron-rich nuclei far from stability and close to the neutron dripline. However, only few of these very exotic nuclei can be produced in current rare isotope beam facilities. Even with next-generation facilities not all nuclei relevant for the *r* process will be reached. In view of the experimental difficulties, calculations based on theoretical models of the reaction chain are essential to understand nucleosynthesis and the origin of the heaviest nuclei in the Universe. Moreover, such calculations are critical to identify key nuclei or regions of nuclei which need to be measured in new radioactive beam experiments.

Even more than the nuclear physics uncertainties, the astrophysical environment of the *r* process is far from understood [1]. The rapidity and the high neutron densities required for this process point to the most neutron-rich objects in the Universe: neutron stars. Many studies have been performed for the high-entropy, neutrino-driven wind subsequent to core-collapse supernovae (see [1] for a review). The conditions necessary for the *r* process have been well established but are not found in recent hydrodynamic simulations [2–5]. The merger of two neutron stars was proposed in [6] and indeed simulations can reach the extreme conditions required for the *r* process (see, e.g., [7,8]). However, neutron star mergers are not occurring early enough in our galaxy to explain the heavy *r*-process elements in very old stars [9].

Typically, the *r* process is modeled taking as theoretical input some scenario of the astrophysical environment together with specific models for nuclei where experimental information is not available. While individual models can be judged by the quality of agreement for the predicted final abundances, the dependence on the nuclear physics entering the different models and which physics features cause discrepancies is not fully understood. The shell effects that cause the abundance peaks can be quenched by different mechanisms. In Ref. [10], the effect of a weakened pairing field in the Hartree-Fock-Bogoliubov (HFB) treatment of nuclei near the dripline was considered. Another mechanism going beyond the correlations treated by HFB will be considered here. It has been found recently that long-range correlations associated with quadrupole degrees of freedom can significantly improve the description of nuclear masses with respect to Hartree-Fock-Bogoliubov (HFB) theory, using either a Skyrme interaction [11] or the Gogny interaction [12]. It was also found that the correlation energy enhances magic number effects at double shell closures and weakens them elsewhere [13], a phenomenon known as ''mutually enhanced magicity'' [14]. The mass table of Ref. [12] contains both the HFB and the correlation contribution permitting us to examine its specific effect on nucleosynthesis. Unfortunately the published table of Ref. [11] was not extensive enough for this purpose.

It should be mentioned that the above HFB model was not tuned to produce accurate mass tables, and in fact does have the overall accuracy achieved by fitted models. Among the most successful is the finite-range liquid drop model [15], which combines phenomenology with a

mean-field contribution estimated by a shell-correction formula. While this model achieves a high overall accuracy, it misses shell closure effects such as the "mutually enhanced magicity" mentioned above and "shell quenching" mentioned in Ref. [16]. Also prominent is the series of models by Goriely and collaborators ([17–19], see cited references), which is a fully microscopic self-consistent mean-field theory with an added phenomenological correlation energy. Clearly, if correlation energies are significant, they should be studied microscopically rather than relying on a simple phenomenological formula. In both Refs. [11,12] the HFB theory was extended by the microscopic generator coordinate method to treat quadrupole correlations, and no parameters were assumed beyond those going into Skyrme or Gogny energy functionals.

Since there is uncertainty about the astrophysical environment of the *r* process, we study the effects of long-range nuclear correlations for the different scenarios mentioned above. Specifically, we consider trajectories arising from hot or cold, high-entropy neutrino-driven winds [2] and from neutron star mergers [20]. In all cases we find that correlations reduce the trough in the abundances before the third *r*-process peak (at $A \approx 195$). Similar reductions have been achieved in nucleosynthesis calculations based on mass models with shell quenching [21]. Here we show that this trough depends not only on the shell closures, but also on the transition from deformed to spherical nuclei. Notice that the behavior of the trough depends on astrophysical conditions and on nuclear physics input. Therefore, proper combination of these both can lead to a good agreement with observations. Our goal here is simply to show relative changes due to correlations, in scenarios that lead to the heavier elements. The impact of the mass models on *r*-process abundances have been extensively discussed; see, e.g., recent works in Refs. [22,23] and references therein.

The most important input to the reaction network from the perspective here is the neutron separation energy, which crucially affects the (γ, n) photodissociation reactions and the (n, γ) capture rates. The separation energies obtained from the mass tables of Delaroche *et al.* [12] are shown in Fig. 1. The left-hand and right-hand panels correspond, respectively, to calculated masses in HFB theory and in their extended theory including correlations. Plotted are contours at constant proton number of half the two-neutron separation energy S_{2n}, as a function of mass number. Delaroche *et al.* [12] calculated only even-even nuclei, so the needed odd-*A* separation energies will be assigned by interpolation. Also, their correlated masses are higher in some nuclei and for those masses we use the HFB values. With the theoretical S_n values, we calculate the neutron-capture cross sections with a simplified Hauser-Feshbach model Eq. (39) in Ref. [24]. The nuclear binding energy differences also affect β-decay rates, but the sensitivity is not as high [23] and we use the table of [16] for these transitions.

We point out two features in the calculated two-neutron separation energies (Fig. 1) that have a major effect on the *r*-process abundances; see also [23] and references therein. First, the abrupt drop of S_{2n} around $A = 130$ and $A = 195$ corresponds to the magic numbers $N = 82$ and $N = 126$, respectively. For these nuclei with closed shells, neutron-capture cross sections are very small and the photodissociation rate is high for typical *r*-process temperatures. As a result the *r*-process path stops at these nuclei and waits for β decay. It is here that matter accumulates and the abundance peaks form, as they are observed in the solar system. The second characteristic feature is the smoothness of the topography just before the magic numbers. Without correlations, the evolution of S_{2n} with *A* shows a pronounced dip just before the $N = 126$ magic number, associated with the transition from deformed to spherical nuclei. This behavior is also present in other mass models [10,15,17].

Nuclear correlations strongly affect these two features. When correlations are included, the neutron shell closures are smoother. The less pronounced drop of S_{2n} at $N = 82$ and $N = 126$ leads to smaller peaks in abundances. The other important effect is the smoothing of the dip in S_{2n} just

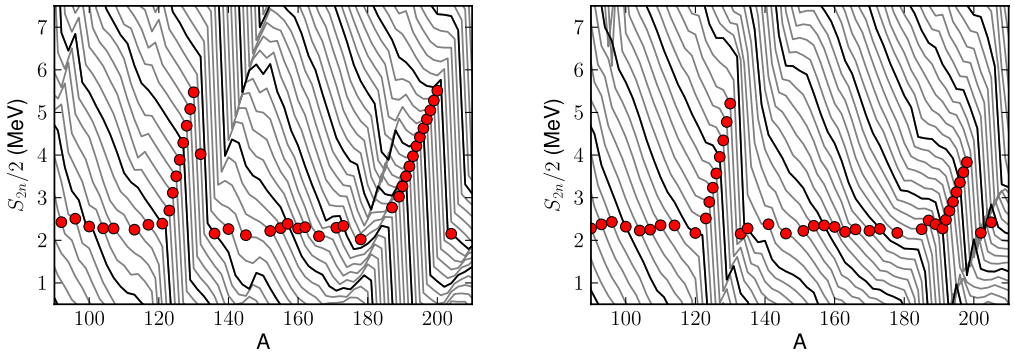

FIG. 1 (color online). Half the two-neutron separation energy $S_{2n}/2$ for constant proton number as a function of mass number *A*. The lines represent isotopic chains from $Z = 30$ to $Z = 80$. The dots mark the *r*-process path for the hot wind trajectory at freeze-out. The left panel corresponds to the nuclear masses of Delaroche *et al.* [12] without nuclear correlations. In the right panel nuclear correlations are included.

before $N = 126$ ($A \approx 180$). This has a big impact on late neutron captures and on the formation and evolution of the trough in the abundances before the $A = 195$ peak.

The evolution of the astrophysical environment is shown in Fig. 2 for the three scenarios we consider. First, we take two trajectories of neutrino-driven wind simulations [2] with the entropy artificially increased to produce the third r-process peak (i.e., the same trajectories as in [23]). The solid black line represents a cold wind evolution where photodissociation is negligible and the evolution is characterized by a competition between neutron captures and β decays. The other trajectory, assuming higher temperatures and densities (dashed green line), is closer to a classical r process [25] in which $(n, \gamma) - (\gamma, n)$ equilibrium is achieved. Moreover, we consider a neutron star merger trajectory (dotted red line) from the simulations of Ref. [20] as applied to the r process (see [7]). Notice the fast drop of the density (initially very high) and the small increase of the temperature (at $t \approx 10^{-2} - 1$ s) due to the energy released by r-process reactions [26].

The resulting abundances are shown in Fig. 3. The nucleosynthesis calculations start at high temperature (~ 1 MeV) with nuclear statistical equilibrium. The initial evolution until charged-particle freeze-out is calculated with a full network of reactions and including nuclei up to $Z = 63$ [23,27]. The r-process phase which follows (after $T \sim 0.25$ MeV) is modeled with a reduced network [23,27] that includes the relevant reactions for the r process (neutron capture, photodissociation, β decay, α decay, and fission). The masses from Ref. [12] are used in this r-process network.

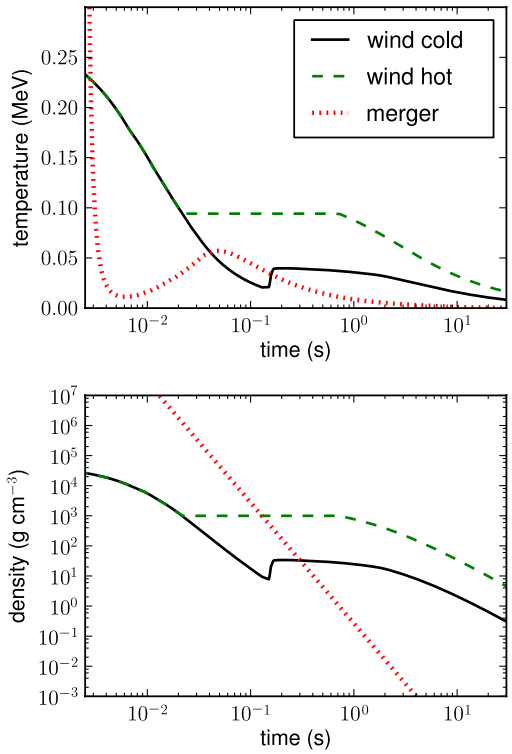

FIG. 2 (color online). Evolution of temperature and density for different astrophysical environments. The trajectories for a neutrino-driven wind with cold (solid black line) and hot (dashed green line) r process are based on the simulations of [2]. The trajectory for the neutron star merger [7] is given by the dotted red line.

The abundances are very different for the three trajectories (see Fig. 3) because they depend very much on the temperature and density evolutions. For example, in the hot wind scenario $(n, \gamma) - (\gamma, n)$ equilibrium is important in determining the abundances. In the other scenarios, the main competition is between neutron captures and β decays. The red dots in Fig. 1 show the r-process path at freeze-out (neutron-to-seed ratio equal one) for the hot wind trajectory. The abundances at this point thus provide crucial information for the r-process phase. Afterwards nuclei β decay to stability, only changing the mass number by β-delayed neutron emission or by capture of the last neutrons (see, e.g., [23,28]). These late-stage reactions lead to the stagger in the resulting abundances between peaks. The observed abundances are much smoother; the difference may be attributed to the approximation used for the neutron captures [23]. This can explain why none of the trajectories produce the rare-earth-element peak ($A \sim 160$) which strongly depends on neutron captures when matter decays to stability [28,29]. None of the scenarios shown here fit the entire range of solar system abundances. Very likely, the observed abundances arise from a superposition of trajectories that individually emphasize the lighter or the heavier mass numbers.

From Fig. 3 one sees that nuclear correlations affect mainly the abundances in the region before the third peak ($180 < A < 190$). Here, the three trajectories show a similar behavior; the correlations reduce the trough. However, the depth of the trough and the impact of correlations depends on the trajectory. For the hot wind (top panel), $(n, \gamma) - (\gamma, n)$ equilibrium is reached and the r-process path is given by the neutron separation energy. Therefore, the features in S_{2n} become crucial to the understanding of the final abundances. The abundances at freeze-out already show a pronounced trough that is reduced and shifted toward higher A during the decay to stability. The evolution and fill-up of the trough therefore depends on neutron captures. These can be enhanced due to the features shown in $S_{2n}/2 \approx 3 - 4$ MeV at $A \approx 180$ without correlations (left panel Fig. 1). For the cold wind (middle panel) the trough and the second peak are smaller than for the hot wind. Because of the lower temperatures during the r process in this case the photodissociation is almost negligible. Therefore, the impact of the masses is smaller as it enters mainly through the neutron captures. The merger trajectory (bottom panel) presents extreme abundances with a very narrow third peak. The dip in S_{2n} increases the neutron captures in the region before the third peak and

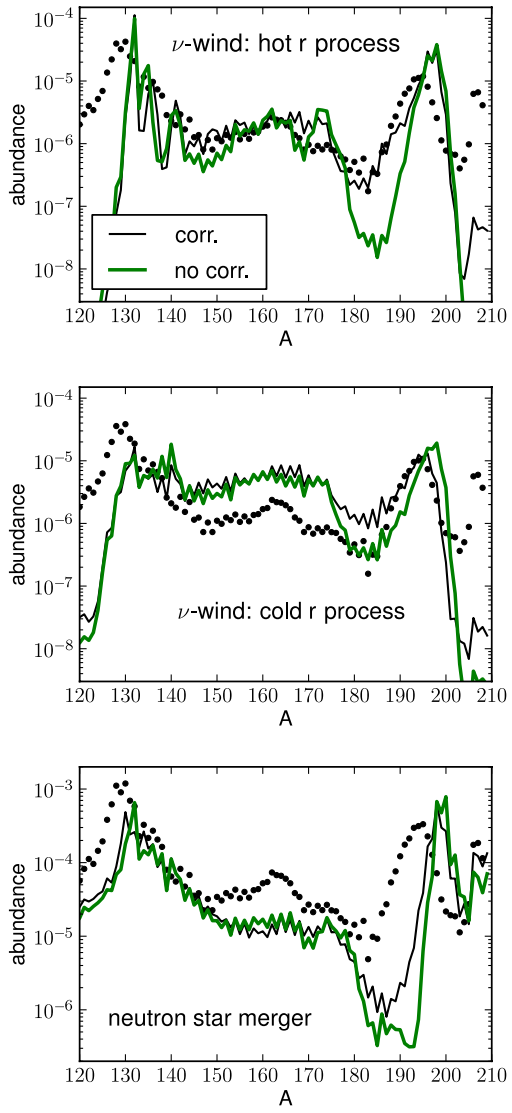

FIG. 3 (color online). Abundances with and without nuclear correlations based on hot and cold wind and neutron star merger trajectories, from the top to the bottom. The black dots are solar system *r*-process abundances.

moves matter towards higher mass numbers. This results in a narrower trough for the calculation with correlations.

In summary, correlations smooth out the nucleus-to-nucleus variations of nuclear separation energies. This is especially pronounced for the region before $N = 126$ as shown by the two-neutron separation energy. The dip observed in S_{2n} without correlations is also present in other mass models [10,15,17] (see Fig. 6 of [23]). In the classical *r* process [25], the problem of the large trough before peaks was previously overcome by quenching the shell gap [21]. The masses of nuclei in the transition region ($180 < A < 190$) between deformed and spherical strongly affect the calculated abundances determining the shape and position of the third peak and the trough before this. We have shown that a microscopic theory of nuclear masses including correlations is sufficient to smoothen the separation energies and thus reduce the trough in the abundances. Our study here shows the strong impact of correlations on *r*-process nucleosynthesis and motivates further theoretical work to treat the nuclear physics as realistically as possible. For the future, we plan to study nucleosynthesis using globally calculated β decays and neutron captures consistently with the theoretical separation energies.

We thank F.-K. Thielemann, G. Martínez-Pinedo, and T. R. Rodríguez for discussions and comments on the manuscript. A. A. was supported by a Feodor Lynen Fellowship of the Alexander von Humboldt Foundation and by the Swiss National Science Foundation. G. F. B. acknowledges support from the U.S. Department of Energy under Grant No. DE-FG02-00ER41132. We also thank the Institute for Nuclear Theory, where this work was initiated. This work has been partially supported by the Helmholtz-University Young Investigator Grant No. VH-NG-825.

*almudena.arcones@physik.tu-darmstadt.de

[1] M. Arnould, S. Goriely, and K. Takahashi, Phys. Rep. **450**, 97 (2007).
[2] A. Arcones, H.-T. Janka, and L. Scheck, Astron. Astrophys. **467**, 1227 (2007).
[3] L. Hüdepohl, B. Müller, H. Janka, A. Marek, and G. G. Raelt, Phys. Rev. Lett. **104**, 251101 (2010).
[4] T. Fischer, S. C. Whitehouse, A. Mezzacappa, F. Thielemann, and M. Liebendorfer, Astron. Astrophys. **517**, A80 (2010).
[5] A. Arcones and H.-T. Janka, Astron. Astrophys. **526**, A160 (2011).
[6] J. M. Lattimer and D. N. Schramm, Astrophys. J. **192**, L145 (1974).
[7] C. Freiburghaus, S. Rosswog, and F.-K. Thielemann, Astrophys. J. **525**, L121 (1999).
[8] S. Goriely, A. Bauswein, and H.-T. Janka, Astrophys. J. **738**, L32 (2011).
[9] D. Argast, M. Samland, F.-K. Thielemann, and Y.-Z. Qian, Astron. Astrophys. **416**, 997 (2004).
[10] J. M. Pearson, R. C. Nayak, and S. Goriely, Phys. Lett. B **387**, 455 (1996).
[11] M. Bender, G. F. Bertsch, and P.-H. Heenen, Phys. Rev. C **73**, 034322 (2006).
[12] J.-P. Delaroche, M. Girod, J. Libert, H. Goutte, S. Hilaire, S. Peru, N. Pillet, and G. F. Bertsch, Phys. Rev. C **81**, 014303 (2010).
[13] M. Bender, G. F. Bertsch, and P.-H. Heenen, Phys. Rev. C **78**, 054312 (2008).
[14] D. Lunney, J. M. Pearson, and C. Thibault, Rev. Mod. Phys. **75**, 1021 (2003).
[15] P. Möller, J. R. Nix, W. D. Myers, and W. J. Swiatecki, At. Data Nucl. Data Tables **59**, 185 (1995).
[16] P. Moller, B. Pfeier, and K.-L. Kratz, Phys. Rev. C **67**, 055802 (2003), see table at http://t16web.lanl.gov/Moller/publications/tpnff.dat.
[17] S. Goriely, N. Chamel, and J. M. Pearson, Phys. Rev. Lett. **102**, 152503 (2009).

[18] S. Goriely, S. Hilaire, M. Girod, and S. Péru, Phys. Rev. Lett. **102**, 242501 (2009).
[19] S. Goriely, N. Chamel, and J. M. Pearson, Phys. Rev. C **82**, 035804 (2010).
[20] S. Rosswog, M. Liebendörfer, F.-K. Thielemann, M. B. Davies, W. Benz, and T. Piran, Astron. Astrophys. **341**, 499 (1999).
[21] B. Chen, J. Dobaczewski, K.-L. Kratz, K. Langanke, B. Pfeier, F.-K. Thielemann, and P. Vogel, Phys. Lett. B **355**, 37 (1995).
[22] K. Farouqi, K.-L. Kratz, B. Pfeier, T. Rauscher, F.-K. Thielemann, and J. W. Truran, Astrophys. J. **712**, 1359 (2010).
[23] A. Arcones and G. Martínez-Pinedo, Phys. Rev. C **83**, 045809 (2011).
[24] S. E. Woosley, W. A. Fowler, J. A. Holmes, and B. A. Zimmerman, California Institute of Technology, W. K. Kellogg Radiation Laboratory, Report No. OAP-422, 1975.
[25] K. Kratz, J. Bitouzet, F. Thielemann, P. Moeller, and B. Pfeier, Astrophys. J. **403**, 216 (1993).
[26] B. D. Metzger, A. Arcones, E. Quataert, and G. Martínez-Pinedo, Mon. Not. R. Astron. Soc. **402**, 2771 (2010).
[27] C. Freiburghaus, J.-F. Rembges, T. Rauscher, E. Kolbe, F.-K. Thielemann, K.-L. Kratz, B. Pfeier, and J. J. Cowan, Astrophys. J. **516**, 381 (1999).
[28] M. Mumpower, G. McLaughlin, and R. Surman, Phys. Rev. C **85**, 045801 (2012).
[29] R. Surman, J. Engel, J. R. Bennett, and B. S. Meyer, Phys. Rev. Lett. **79**, 1809 (1997).